

## Buck-Converter Photovoltaic Simulator

F. Yusivar, M. Y. Farabi, R. Suryadiningrat, W. W. Ananduta, and Y. Syaifudin.

Electrical Engineering Department, Universitas Indonesia.  
Kampus Baru UI Depok 16424, telp:62-21-7270078/fax:62-21-7270077  
e-mail: yusivar@ieee.org

### Abstract

*This paper presents a Photovoltaic Simulator Simulation using Buck Converter with analysis using bode diagram. A state space simulator model is derived to provide a detail non-linear model. The PV Static Model is modified by adding a low pass filter in order to avoid an algebraic loop problem and able to analyze easier. PV simulator is realized by controlling buck converter's current using PI Controller with reference from PV model. Then the model is linearized which is used for analysis purpose. The system is analyzed using bode diagram for its output voltage against its inputs of solar irradiance and cell's temperature. The Load, Proportional Gain  $K_p$ , and Integral Gain  $K_i$  are varied to observe their effects into the system stability. It is noticed that the limits of gain stability system are so high at all values of load and gains so the Buck-Converter Photovoltaic Simulator, which is proposed here, can be declared as a robust system.*

**Keywords:** Photovoltaic simulator, buck converter, simulation analysis, stability.

### 1. Introduction

Solar cell is a solid state device that converts the energy of sunlight directly into electricity by the photovoltaic effect. Solar cell has a few advantages such as pollution-free, low maintenance costs, as well as low operating costs. However, the efficiency of the solar cell itself is still very small. Many factors affect the performance of the solar. Therefore simulation is needed to find out how much these factors affect the performance of the solar cell [1]~[5].

A Photovoltaic (PV) Simulator can be found in many different ways. Some simulators are implemented using experimental PV equivalent circuit with diodes [6], some with DSP Controller [7], and others are simulate only the I-V curves of PV characteristics [8]. However, the simulator using experimental PV equivalent circuit with diodes [6] uses the short circuit current to be its input, not the real inputs of the solar cell: solar irradiance ( $\lambda$ ) and cell's temperature ( $T_c$ ). The PV equivalent circuit should be replaced with the derived equation from simulation of I-V curves of PV characteristics [8]. This model is called PV Static Model, since it use a straight mathematic input-output relation to make the simulator resembles the actual solar cell. With using the PV Static Model, one could has an algebraic loop problem since the output is looped back to calculate the output itself. Furthermore, this problem also cause a difficulty to derived the model for simulation and analysis purposes. In order to overcome this problem, a low pass filter is added to cut the algebraic loop, and then the model is easy to be realized and analyzed. Here, the modified model is called the PV dynamic model. The PV simulator is realized by a buck converter, with PI controller and PWM generator.

In this paper, a simulation of photovoltaic is designed with using a DC-DC converter. A buck converter will be used and is current controlled by PI controller with PWM generator to regulate the power switch [10]-[11]. The PV characteristics are implemented using PV Static Model and uses a Low-Pass Filter to turn the static model into a dynamic model of photovoltaic characteristics. The inputs for the system are solar irradiance and cell's temperature. The system then will be analyzed with bode diagram for its voltage output against its two inputs: solar irradiance ( $\lambda$ ) and cell's temperature ( $T_c$ ).

### 2. Research Method

The purpose of research is to find an easy way to simulate and analyze a PV simulator system. A modified PV model is proposed by adding a low pass filter into a PV static model. The research method is divided into three steps. First, the modified PV simulator model is derived. The model is a detail non-linear state space model which is used for simulation. The second step is to linearized the model since then it can be used for analysing the system using a classic method such as Bode plot analysis. In the last step, the whole system of PV simulator is analyzed using a Bode plot.

#### 2.1. Simulator Model

The designed circuit is buck converter which outputs a voltage source with the output current is controlled to create current as its reference determined by the PV model. Figure 1 shows the PV simulator block diagram. As shown in the figure, the PV static model requires voltage and current information inputs to calculate the current

reference  $I_{ref}$ . If  $I_{ref}$  is used for this purpose and with a low pass filter is inserted, there will be an algebraic loop. Although, one can use the current information from the buck converter (I), it will cause degradation in the dynamic behavior of the system since this current is also used as the feedback for current PI controller. Therefore, inserting a low pass filter between PV Static Model output and its feedback will overcome the problem.

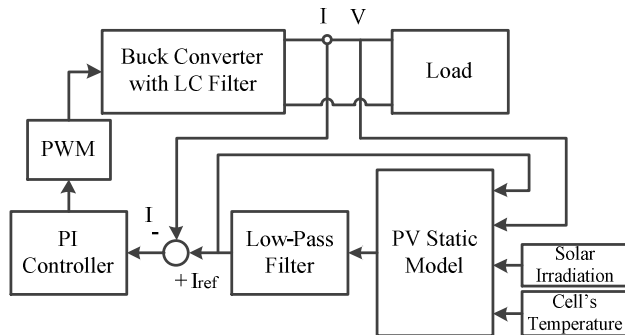


Figure 1. PV simulator block diagram.

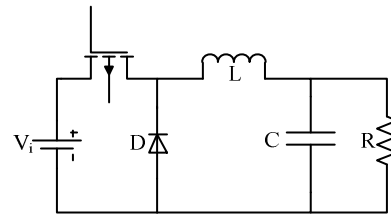


Figure 2. Buck Converter Circuit

On the blocks, there are several blocks which have own function. The buck converter is characterized by buck converter with LC filter block and load block. A single stage LC filter will be used so only one inductor and one capacitor exist in the circuit. A  $21 \mu F$  capacitor and a 3mH inductor are used in the circuit. Figure 2 shows the buck converter circuit with its load. The voltage generated from the buck converter will be detected and input to PV Static Model to generate the current reference of PV Static Model by following the low pass filter. Voltage that'll be referenced to the PV Static Model is the output voltage measured at load R. Then, a low-pass filter is used to get the response time for the current reference before it works in its own steady state. This turns the PV Static Model into a dynamic model. The output from low-pass filter will be used for reference to control the buck's current.

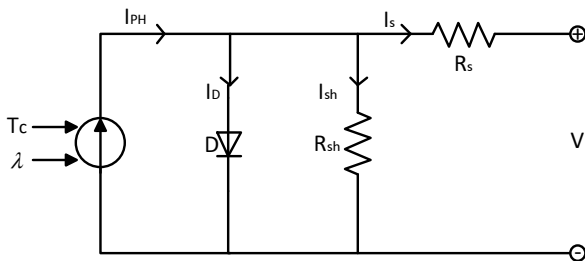


Figure 3. Photovoltaic equivalent circuit.

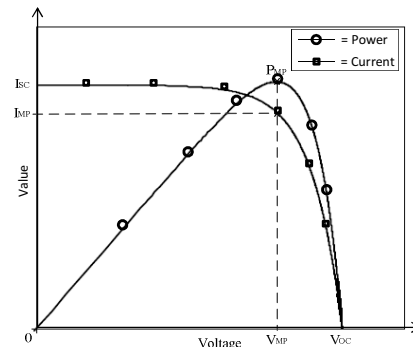


Figure 4. PV characteristics

Figure 3 shows the equivalent circuit of photovoltaic. Most of photovoltaic simulation was made to simulate the characteristics of the relationship between the current and the voltage of photovoltaic. Figure 4 shows the characteristic graph of relationship between current and voltage of the photovoltaic, and the power generated from these two relationships. With the increase of the voltage, then the current will be reduced until a condition of open circuit ( $I=0$ ). From these relationship, there will be a point where the value of voltage and current that will generate the maximum power, or known as MPP (Maximum Power Point). The technique, used in order to maintain the power to always be at the maximum point, is commonly known as MPPT (Maximum Power Point Tracker). The MPPT is not implemented and simulated in the system, since the purpose of this research is only for the PV simulator.

The voltage from buck converter will be used as input to the PV model to simulate the characteristic of photovoltaic. Because the input is a voltage, the one that will be controlled is the current and it will be controlled by PI controller and generate PWM pulse on the next block. PV Static model is needed to create the reference current. It contains equations with the solar irradiance and cell's temperature as inputs. From the equivalent circuit in Fig. 3, the characteristics equation for PV Static Model derived as:

$$I = I_{PH} - I_D - I_{R_{sh}} = I_{PH} - I_{RS} \left( \exp \left( \frac{q \left( \frac{V}{N_s} + IR_s \right)}{nkT_c} \right) - 1 \right) - \frac{V}{N_s} + IR_s \quad (1)$$

where:

- $I_{PH}$  = photovoltaic current
- $I_D$  = diode's current
- $I_{sh}$  = shunt resistor's current
- $I_{RS}$  = dark saturation current
- $q$  = electron =  $1.6 \times 10^{-19} C$
- $V$  = voltage
- $R_s$  = series resistance
- $n$  = ideal factor
- $k$  = Boltzmann's constant =  $1.38 \times 10^{-23} J / K$
- $T_c$  = cell temperature
- $R_{sh}$  = shunt resistance
- $N_s$  = number of series solar cells

From Eq. (1), a block of PV Static Model is derived with inputs of voltage reference from buck converter, solar irradiance, and cell's temperature, and the current to output a current. It uses a current to calculate the current (algebraic loop). By adding a low pass filter, the current reference used to control the buck's current is obtained without an algebraic loop problem.

The PV Static Model needs to be converted into a dynamic model by added a low-pass filter. The transfer function of low-pass filter is as follow:

$$\frac{output}{input} = \frac{I_{LPF}(s)}{I_{PV}(s)} = k \frac{1}{Ts + 1}$$

With the low-pass filter is used, Eq. (1) becomes:

$$I = I_{PH} - I_{RS} \left( \exp \left( \frac{q \left( \frac{V}{N_s} + I_{LPF} R_s \right)}{nkT_c} \right) - 1 \right) - \frac{V}{N_s} + I_{LPF} R_s \quad (2)$$

where:

- $I_{LPF}$  = low-pass filter's current.

This characteristic equation is completed by the following equations:

$$\begin{aligned} V_{OC} &= V_{OC-STC} + \beta(T - T_{ref}) \\ I_{SC} &= \frac{\lambda}{\lambda_{ref}} I_{SC-STC} \\ I_{PH} &= I_{sc} \frac{\lambda}{\lambda_{ref}} + \alpha(T_c - T_{ref}) \\ I_{RS} &= \frac{I_{sc}}{\left( \exp \frac{qV_{oc}}{nkT_{ref}} - 1 \right)} \end{aligned}$$

where:

- $\lambda$  = solar irradiance
- $\lambda_{ref}$  = solar irradiance's reference =  $1000 W/m^2$

- $\alpha$  = temperature coefficient of  $I_{sc}$
- $I_{RS}$  = dark saturation current
- $I_{SC}$  = short circuit current
- $V_{OC}$  = open circuit voltage
- $q$  = electron= $1.6 \times 10^{-19} C$
- $n$  = ideal factor
- $k$  = Boltzmann's constant= $1.38 \times 10^{-23} J / K$
- $T_{ref}$  = temperature reference= $25^{\circ}C=298 K$
- $I_{SC-STC}$  = short circuit current at Standard Test Condition
- $V_{OC-STC}$  = open circuit voltage at Standard Test Condition
- $I_s$  = solar cell's saturation current

The other parameters those have not been defined in above equations, are adopted from parameters of KC50T Kyocera solar cell and listed in Table 1. The value of series and shunt resistances ( $R_s = 0.691$  ohm and  $R_{sh} = 10850$  ohm) are adopted from [11]. Cell's temperature and solar irradiance will be the inputs for this system, so their value can be varied and analyzed then.

Table 1. Solar Cell KC50T Parameters.

Characteristics	Value
Rated Power, Watts (Pmax)	54 + 10% -5%
Open Circuit Voltage (Voc)	21.7
Short Circuit current (Isc)	3.31
Voltage at Load (Vpm)	17.4
Current at Load (Ipm)	3.11
Temp. coefficient of Voc (V/°C)	$-8.21 \times 10^{-2}$
Temp. coefficient of Isc (A/°C)	$1.33 \times 10^{-3}$
Temp. coefficient of Vpm (V/°C)	$-9.32 \times 10^{-2}$

After the system has been designed, the system is then modeled to the mathematical. The block diagram of the whole system with including the Modified PV model is shown in Fig. 5, and its transfer function block diagram is in Fig. 6.

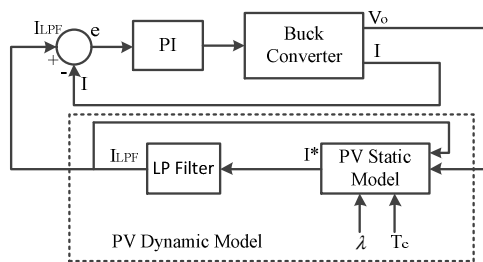


Figure 5. The modified PV simulator.

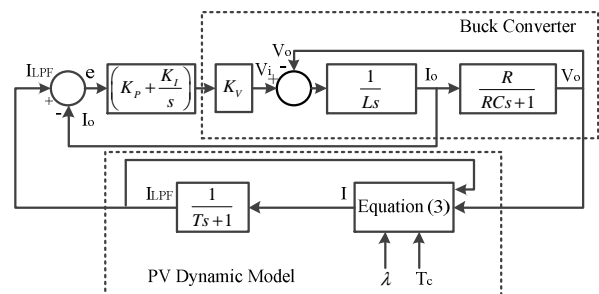


Figure 6. Transfer Function Block Diagram of Buck Converter PV-Simulator.

$$I = I_{PH} - I_{RS} \left( \exp \left( \frac{q \left( \frac{V_o}{N_s} + I_{LPF} R_s \right)}{nkT_c} \right) - 1 \right) - \frac{V_o + I_{LPF} R_s}{R_{sh}} \quad (3)$$

The PWM generator is assumed as ideal gain system. In this paper, the duty cycle of the PWM output will be multiplied with gain  $K_v$  (value of DC voltage in buck converter). The buck converter with a PI control systems model are easily derived based on the block diagram in Fig. 6. After the system's been modeled, the differential equation of the whole system can be obtained. The non-linear model of the system is described in differential equations of Eqs. (4)~(7).

$$\frac{d}{dt} X_{PI} = I_{LPF} - I \quad (4)$$

$$\frac{d}{dt} I = \frac{K_v K_p}{L} I_{LPF} - \frac{K_v K_p}{L} I + \frac{K_v K_I}{L} X_{PI} - \frac{1}{L} V_o \quad (5)$$

$$\frac{d}{dt} V_o = -\frac{1}{RC} V_o + \frac{1}{C} I \quad (6)$$

$$\frac{d}{dt} I_{LPF} = -\frac{1}{T} I_{LPF} + \frac{1}{T} I^* \quad (7)$$

where:

$$I^* = \left( \frac{\lambda}{\lambda_{ref}} I_{SC-STC} + \alpha(T_c - T_{ref}) \right) - \frac{V}{N_s} + \frac{R_s I_{LPF}}{R_{sh}} - \left( \frac{I_{sc-stc} \left( \frac{T_c}{T_{ref}} \right)^3}{\left( \exp \frac{qV_{oc}}{nkT_{ref}} - 1 \right)} \right) \left( \exp \frac{qE_g \left( \frac{1}{T_{ref}} - \frac{1}{T_c} \right)}{nk} \right) \left( \exp \frac{q \left( \frac{V}{N_s} + I_{LPF} R_s \right)}{nkT_c} - 1 \right)$$

## 2.2. Linearization

For analysis purpose, those non-linear equations are needed to be linearized. The Euler method is used for linearization. The linearized model of PV simulator are written in Eqs. (8)~(11).

$$\frac{d}{dt} \Delta X_{PI} = \Delta I_{LPF} - \Delta I \quad (8)$$

$$\frac{d}{dt} \Delta I = \frac{K_v K_p}{L} \Delta I_{LPF} - \frac{K_v K_p}{L} \Delta I + \frac{K_v K_I}{L} \Delta X_{PI} - \frac{1}{L} \Delta V_o \quad (9)$$

$$\frac{d}{dt} \Delta V_o = -\frac{1}{RC} \Delta V_o + \frac{1}{C} \Delta I \quad (10)$$

$$\begin{aligned} \frac{d}{dt} \Delta I_{LPF} = & \left( -\frac{1}{T} - \frac{1}{T} \left( \frac{R_s}{R_{sh}} + \left( \frac{qR_s I_{RS} T_{c0}^2}{nkT_{ref}^3} \right) A_1 A_2 \right) \right) \Delta I_{LPF} + \left( \frac{\alpha}{T} + \frac{T_{c0} I_{RS} A_1}{TT_{ref}^3} \left( 3T_{c0} - \frac{qE_g}{nk} + A_2 A_3 \right) \right) \Delta T_c \\ & + \frac{1}{T} \left( \frac{1}{N_s R_{sh}} - \left( \frac{qI_{RS} T_{c0}^2}{nkN_s T_{ref}^3} \right) A_1 A_2 \right) \Delta V_o + \frac{1}{T} \left( \frac{I_{SC-STC}}{\lambda_{ref}} \right) \Delta \lambda \end{aligned} \quad (11)$$

where:

$$A_1 = \exp \left( \frac{qE_g \left( \frac{1}{T_{ref}} - \frac{1}{T_{c0}} \right)}{nk} \right)$$

$$A_2 = \exp\left(\frac{q\left(\frac{V_{o0}}{N_s} + I_{LPF0}R_s\right)}{nkT_{c0}}\right)$$

$$A_3 = \left(3T_{c0} + \frac{q}{nk}\left(E_g - \left(\frac{V_{o0}}{N_s} + I_{LPF0}R_s\right)\right)\right)$$

### 2.3. Bode plot

Bode plot is a sinusoidal transfer function which consists of two separate graphs. One is a diagram of sinusoidal logarithmic transfer function (magnitude) and another is the phase angle. Both graphs are drawn versus frequency in logarithmic scale. From the linearized model of Eqs. (8)~(11), the state space model can be obtained in the general model:

$$\dot{x} = Ax + Bu \quad (12)$$

$$y = Cx + Du \quad (13)$$

with four states of  $\Delta X_{PI}$ ,  $\Delta I$ ,  $\Delta V$ , and  $\Delta I_{LPF}$ , and inputs are solar irradiance ( $\lambda$ ) and cell's temperature ( $T_c$ ). The matrix A, B, C, and D for state space is as follows:

$$A = \begin{bmatrix} 0 & -1 & 0 & 1 \\ \frac{K_v K_i}{L} & -\frac{K_v K_p}{L} & -\frac{1}{L} & \frac{K_v K_p}{L} \\ 0 & \frac{1}{C} & -\frac{1}{RC} & 0 \\ 0 & 0 & A_{43} & A_{44} \end{bmatrix}$$

$$B = \begin{bmatrix} 0 & 0 \\ 0 & 0 \\ 0 & 0 \\ \frac{1}{T}\left(\frac{I_{SC-STC}}{\lambda_{ref}}\right) & B_{42} \end{bmatrix},$$

$$C = [0 \quad 0 \quad 1 \quad 0],$$

$$D = [0 \quad 0]$$

where:

$$A_{43} = \frac{1}{T}\left(\frac{1}{N_s R_{sh}} - \left(\frac{q I_{RS} T_{c0}^2}{nk N_s T_{ref}^3}\right) A_1 A_2\right)$$

$$A_{44} = \left(-\frac{1}{T} - \frac{1}{T}\left(\frac{R_s}{R_{sh}} + \left(\frac{q R_s I_{RS} T_{c0}^2}{nk T_{ref}^3}\right) A_1 A_2\right)\right)$$

$$B_{42} = \left( \frac{\alpha}{T} + \frac{T_{c0} I_{RS} A_1}{TT_{ref}^3} \left( 3T_{c0} - \frac{qE_g}{nk} + A_2 A_3 \right) \right)$$

To be able to create bode plot from state space, it is necessary to convert it into a closed loop transfer function with using the following equation:

$$G_c(s) = C(sI - A)^{-1} B + D \tag{14}$$

Then the closed loop transfer function is converted into open loop transfer function by the following equation:

$$G_o(s) = \frac{G_c(s)}{1 - G_c(s)} \tag{15}$$

The bode plot of open loop transfer function is then used to analyze the stability of PV simulator. The effect of the value of gain's controller against the load on the buck converter will be analyzed. The best value of  $K_p$  and  $K_i$  are needed to be obtained first through a trial and error method. Then the load will be varied and the system can be analyzed.

### 3. Results and Analysis

In this section, the system will be analyzed. First of all, the system is verified if it resembles the actual solar cell by varying the value of load. If the graph resembles the characteristic of photovoltaic, so the designed simulation is well made. It uses 15 units of solar cells arranged in series with load change from 50 ohm to 150 ohm.

Table 2. Simulation Results of the System with Load Changes

Load (Ohm)	Voltage (Volt)	Current (Ampere)	Power (Watt)
50	164.3350	3.2867	540.1198
60	196.8900	3.2815	646.0945
70	228.9560	3.2708	748.8693
80	255.3440	3.1918	815.0069
85	263.6275	3.1015	817.6407
90	269.5320	2.9948	807.1944
100	277.5700	2.7757	770.4510
110	283.0740	2.5734	728.4626
120	287.2200	2.3935	687.4611
130	290.5110	2.2347	649.2049
140	293.2300	2.0945	614.1702
150	295.5300	1.9702	582.2532

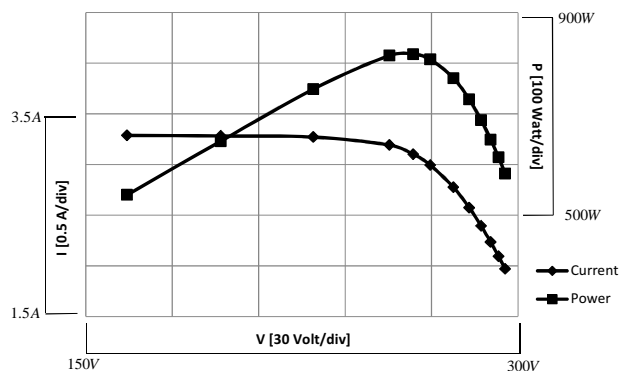


Figure 7. Photovoltaic Characteristic derived from simulation: current vs voltage, and power vs voltage.

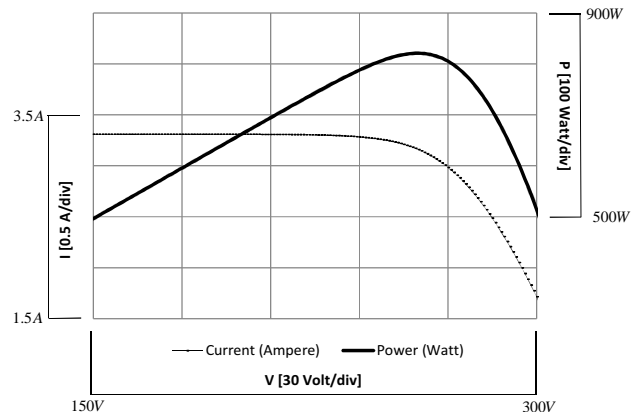


Figure 8. The ideal characteristic of solar cell Kyocera KC50T

The steady state values of voltage, current, and Power of PV simulator with variation on load are listed in Table 2. The I-V and P-V characteristics are plotted and can be viewed in Fig. 7. The ideal graph of solar cell Kyocera KC50T, calculated using Eq. (1), is shown in Fig. 8. From Fig 7, it can be seen that the graph is similar to Fig 8, so the simulation resembles the ideal solar cell Kyocera KC50T.

The effect of input solar cells to the output current will be analyzed. In this simulation, there are two inputs, namely solar irradiance and temperature of solar cells. The solar irradiance will be dropped from 1000 W/m<sup>2</sup> to 600 W/m<sup>2</sup> and the cell's temperature will be dropped from 40<sup>0</sup>C to 27<sup>0</sup>C. The simulation results can be viewed in Fig. 9.

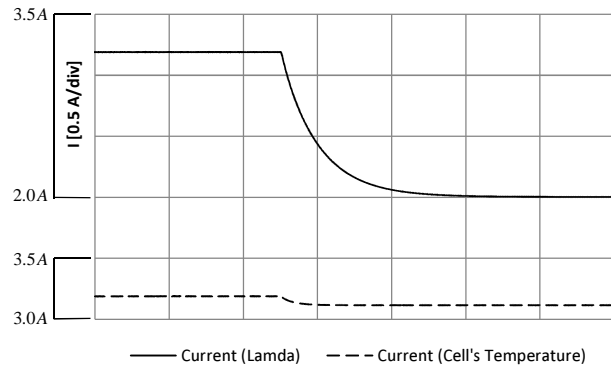


Figure 9. Simulation results of PV current when solar irradiance and cell's temperature are changed.

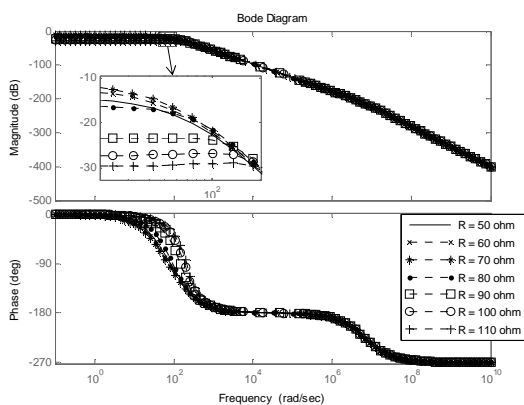


Figure 10. Bode plot of voltage against  $\Delta\lambda$  which load is varied.

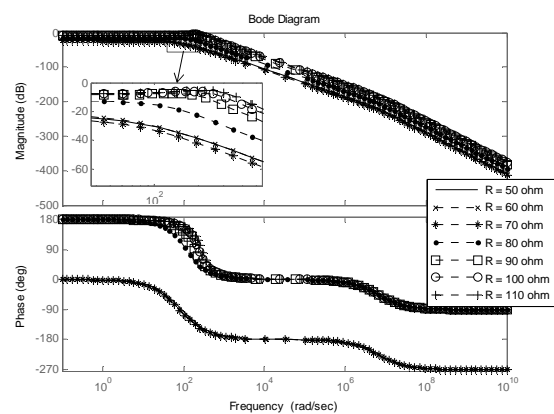


Figure 11. Bode plot of voltage against  $\Delta T_c$  which load is varied.

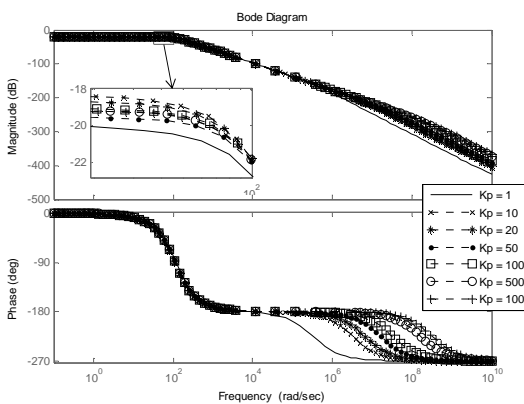


Figure 12. Bode plot of voltage against  $\Delta\lambda$  which  $K_p$  is varied

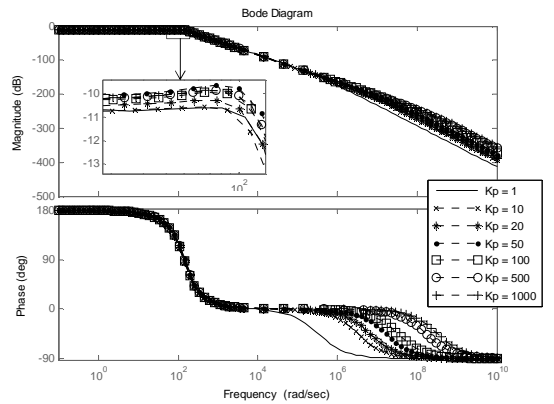


Figure 13. Bode plot of voltage against  $\Delta T_c$  which  $K_p$  is varied

From Fig. 9, when the solar irradiance drops from 1000 W/m<sup>2</sup> to 600 W/m<sup>2</sup>, the output's current will be dropped about 1.5A while with the dropped cell's only about 0.1A. From this point of view, it can be concluded that



the solar irradiance's changes will affect the current's output more significant than the cell has.

In order to analyze the system stability then bode diagram of the open loop system is plotted with the varied value of load and constant values of  $K_p=20$  and  $K_i=10$ . The load is varied from 50 ohm to 110 ohm with the increase of 10 ohm. Figures 10 and 11 show the bode plot of  $\Delta V$  with solar irradiance and cell's temperature as inputs respectively.

Figures 10 and 11 show that if the load is increased, the magnitude will be higher, and at one point of load, it will be the point that has the highest gain margin, and then if load is increased more, the gain margin will be decreased. We can conclude that the load changes affect the frequency responses of system significantly. Overall, with the load changes, the system is stable because the gain margins are always positive.

Then the bode diagram is plotted with the system's conditions: a constant value of load  $R=85$  ohm, the varied values of  $K_p$  are 1, 10, 20, 50, 100, 500, 1000, and a constant value of  $K_i=10$ . Figures 12 and 13 show the bode plot for solar irradiance and cell's temperature inputs respectively. Figure 12 and Figure 13 show how the change of  $K_p$  affect the frequency responses of system. From both figures, it can be seen that the higher the  $K_p$ , the gain margin will be reduced although the effect is relative small. So  $K_p$  changes only affect the system relatively small compared to the load changes. Overall, the system is stable because the gain margins are positive.

Furthermore, bode diagram is plotted for the varied value of  $K_i$  (1, 10, 20, 50, 100, 500, 1000), with the constant values of  $K_p=20$  and load  $R=85$  ohm. Figures 14 and 15 show the bode plot of  $\Delta V$  with solar irradiance and cell's temperature as inputs respectively. From Figs. 14 and 15, for solar irradiance and cell's temperature inputs, with the increases value of  $K_i$ , the magnitude's frequency response of the system are almost same. Overall, the system is stable because the phase margins are positive. From bode plot, it can be seen that the changes of load affect the system more significant than the changes of  $K_p$  and  $K_i$ . So the effect of load changes need to be analyzed more using root locus method. Using root locus plot, the gain limit of stability can be defined easier than using bode plot.

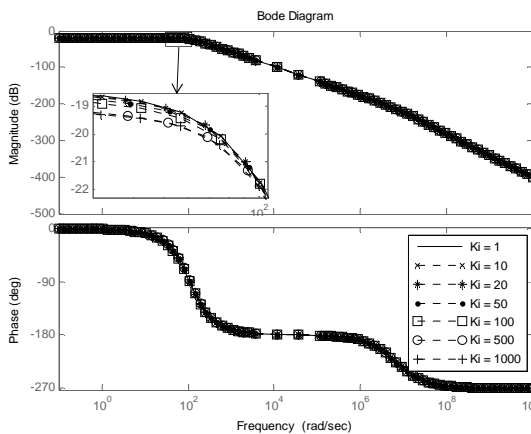


Figure 14. Bode plot of voltage against  $\Delta \lambda$  which  $K_i$  is varied

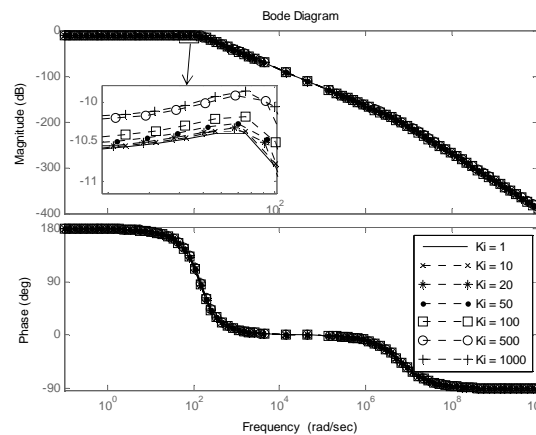


Figure 15. Bode plot of voltage against  $\Delta T_c$  which  $K_i$  is varied

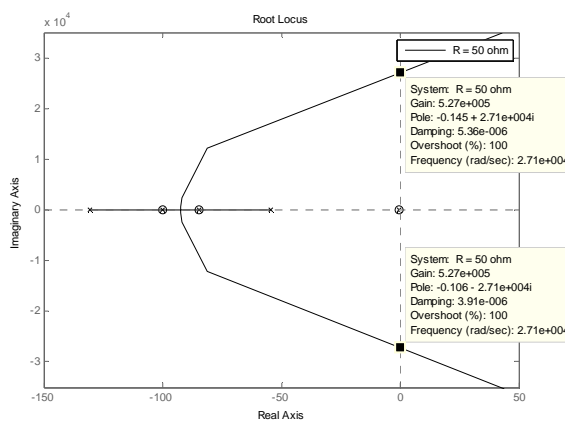


Figure 16. Root locus plot of the system against  $\Delta \lambda$  which load is 50 ohm

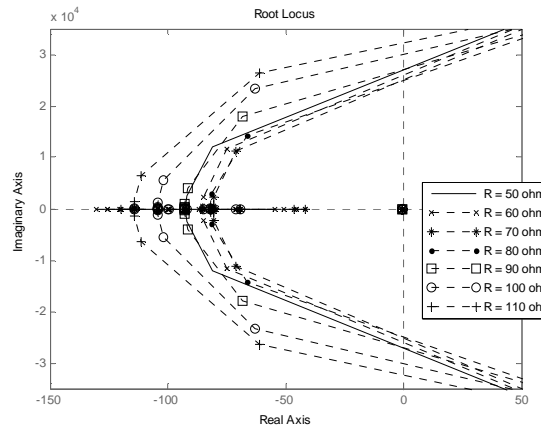


Fig 17. Root locus plot of the system against  $\Delta \lambda$  which load is varied

Figure 16 shows the root locus plot of system's voltage against  $\Delta\lambda$  which load is 50 ohm,  $K_p=20$ , and  $K_i=10$ . It can be seen that the system will be unstable for gain greater than  $5.27 \times 10^5$ . But this value of gain is so high, so the system can be stated as a stable system.

Figure 17 shows the root locus plot of system's voltage against  $\Delta\lambda$  which load is varied from 50 ohm until 110 ohm. The gain stability limit for each load condition is plot in Fig. 18. It can be seen that the system has minimum gain stability limit of about  $4.5 \times 10^5$  at the load of around 80 ohm. However, since the gain stability limits are so high in order of  $10^5$ , it can be concluded that in general the system is stable.

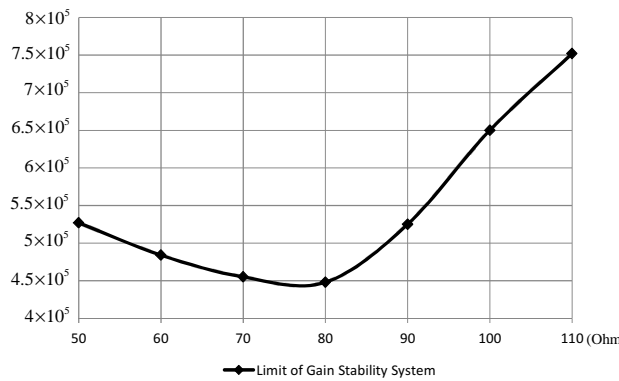


Figure 18. Gain stability limit versus load

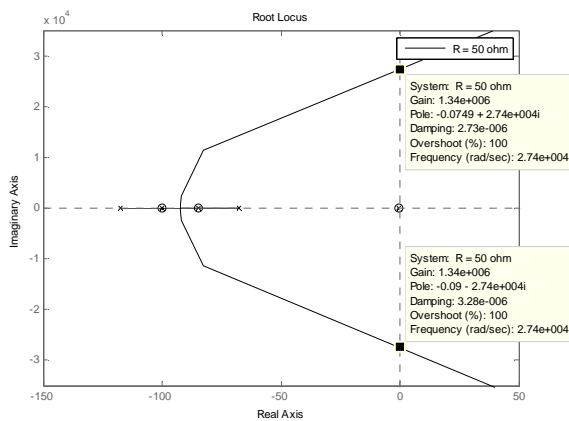


Figure 19. Root locus plot of the system against  $\Delta T_c$  which load is 50 ohm

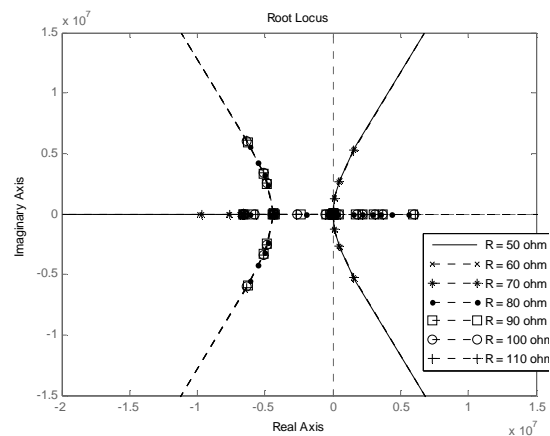


Figure 20. Root locus plot of the system against  $\Delta T_c$  which load is varied

Figure 19 shows root locus of the system against  $\Delta T_c$  which load is 50 ohm,  $K_p=20$ , and  $K_i=10$ . The system becomes unstable for gain greater than  $1.34 \times 10^6$ . But this value of gain is so high, so the system can be stated as a stable system. Figure 20 shows root locus of the system against  $\Delta T_c$  which load is varied. In this case, the gain stability limit are also so high about  $1.34 \times 10^6$ ,  $1.25 \times 10^6$ , and  $1.94 \times 10^6$  for its value of load of 50, 60, and 70 ohms respectively. If the load is increased more, the system will always be on the left side of imaginary axis that means the system should always be stable.

#### 4. Conclusion

A PV simulator's been designed in order to be simulated and analyzed. PV characteristic graph can be plotted from simulation result with the value change of load. The cell's temperature affects the output system, but is less significant compared to the solar irradiance does. The higher the solar irradiance, the greater the output's current.

The PV dynamic model is proposed which is composed from its static model and a low pass filter. The non-linear model of PV simulator has been derived for simulation purpose, and it has been linearized for analysis purpose. From bode plot analysis, it is noticed that load's changes affect the system significantly. However, The constants of PI controller ( $K_p$  and  $K_i$ ) have not effect to the system significantly compared to the load has. Because

the gain margins are always positive, the PV simulator can be declared as a stable system.

From root locus, it is noticed that the gain stability limit of system is so high in order of  $10^5$  for  $\Delta\lambda$  input and  $10^6$  for  $\Delta T_c$  input, so the proposed PV simulator system is a robust system.

## References

- [1] D. L. King, B. R. Hansen, J. A. Kratochvil, and M. A. Quintana, "Dark Current-Voltage Measurements on Photovoltaic Modules as a Diagnostic or Manufacturing Tool," *the 26th IEEE Photovoltaic Specialists Conference*, September 29-October 3, 1997, Anaheim, California, 1997.
- [2] F. M. González-Longatt, "Model of Photovoltaic Module in Matlab™," in *II CIBELEC 2005*, 2005.
- [3] T. Marnoto, K. Sopian, W. R. W. Daud, M. Algoul, and A. Zaharim, "Mathematical Model for Determining the Performance Characteristics of Multi-Crystalline Photovoltaic Modules," *Proc. of the 9th WSEAS Int. Conf. on Mathematical and Computational Methods in Science and Engineering*, Trinidad and Tobago, November 5-7, 2007, pp. 79-84, 2007.
- [4] F. Adamo, F. Attivissimo, A. Nisio, A. Lanzolla, and M. Spadavecchia, "PARAMETERS ESTIMATION FOR A MODEL OF PHOTOVOLTAIC PANELS," in *2009 XIX IMEKO World Congress Fundamental and Applied Metrology*, pp. 964-967, 2009.
- [5] I. H. Atlas, and A. M. Sharaf, "A Photovoltaic Array Simulation Model for Matlab-Simulink GUI Environment," in *2007 International Conference on Clean Electrical Power*, pp.341-345, 2007.
- [6] A. Koran, K. Sano, R.-Y. Kim, and J.-S. Lai, "Design of a Photovoltaic Simulator with a Novel Reference Signal Generator and Two-Stage LC Output Filter," in *Energy Conversion Congress and Exposition, 2009. ECCE 2009. IEEE*, pp. 319-326, 2009.
- [7] Y. Li, T. Lee, F. Z. Peng, and D. Liu, "A Hybrid Control Strategy for Photovoltaic Simulator," in *Applied Power Electronics Conference and Exposition, 2009. Twenty-Fourth Annual IEEE*, pp.899-903, 2009.
- [8] H.-L. Tsai, C.-S. Tu, and Y.-J. Su, "Development of Generalized Photovoltaic Model Using MATLAB/SIMULINK," *Proceedings of the World Congress on Engineering and Computer Science 2008 San Francisco*, 2008.
- [9] N. P. R. Iyer, and V. Ramaswamy, "MODELING AND SIMULATION OF A SWITCHED MODE POWER SUPPLY USING SIMULINK," *University of Technology Sydney*, 2007.
- [10] Gunawan and F. Yusivar, "Design of DC-DC Buck Converter using discrete PID control as output voltage controller," *Final Project Electrical Engineering, Universitas Indonesia*, 2009.
- [11] L. K. Lin, "A Hybrid Wind/Solar Energy Converter," *SIM University*, 2009.

## Bibliography of authors



**Feri Yusivar** was born in Bandung, Indonesia. He received his Bachelor degree in Electrical Engineering at Universitas Indonesia in 1992, and completed his Doctor degree in 2003 at Waseda University, Japan. He is currently the Head of Control Laboratory in Electrical Engineering at Universitas Indonesia. His research interests are control system, electrical drive, power electronics, and renewable energy.



**Muhamad Yasil Farabi** was born in Jakarta in 1990. He received the S.T. degrees in 2011, from Universitas Indonesia, Depok, Indonesia, majoring in electrical engineering



**Rian Suryadiningrat** was born in Kuningan, Indonesia. He received the S.T degree in electrical engineering from Universitas Indonesia (UI), Depok, Indonesia in 2011. During studied in university, he had ever joined in research group student in electronic and control system. His research interests are power control and renewable energy.



**Wayan Wicak Ananduta** was born in Denpasar May 8th 1990. He received the B.Eng degree in electrical engineering from University of Indonesia in 2011. His area of interest for research is in power electronic, control system, and renewable energy.



**Yuddy Syaifudin** received S.T. (Sarjana Teknik, equivalent to Bachelor of Engineering) in electrical engineering from the Electrical Engineering Department, Engineering Faculty, Universitas Indonesia (University of Indonesia) in 2011. He was joined as Control Engineering Laboratory Assistant Team in the university in 2009. Besides, he was joined as Real Time Measurement and Control Research Group in the university in 2011. His thesis, entitled Performance Enhancement of Digital Phase Locked Loop Algorithm in Synchronizing the Waveform on Grid Connected Photovoltaic System, shows his interest in electrical power system and their control system.